High-granularity charge readout of Micro-Pattern Gaseous Detectors with the Timepix4

Summer student report

Zoe Richardson
On behalf of CERN EP-DT-DD GDD team

Supervisors: Lucian Scharenberg, Florian Brunbauer

September 4, 2024

Abstract

When Micro-Pattern Gaseous Detectors (MPGDs) are combined with pixelated readout systems, the benefits of both can be utilised together, for example the low material budget of the gaseous detectors and the high spatial accuracy of the pixelated readout system. The goal of this project was to take steps towards combining a specific version of each: the micro Resistive Well (microRWELL) MPGD with the Timepix4 front-end ASIC. This has been undertaken by first analysing silicon data with features similar to the data recorded with a gaseous detector with the existing silicon sensor clustering software to check how the reconstruction will work for gaseous detector signals. Afterwards, the detector electronics integration was started. First, with a triple-GEM detector, as it was proven to work well with previous versions of the Timepix. X-ray images were obtained successfully. And finally simulating the charge coupling from the microRWELL to the readout pads showed that the coupling behaves qualitatively in the way it was expected to. From these tests, it has been concluded that the assembly process with the microRWELL and Timepix4 with Through Silicon Via (TSV) should be further pursued.

Contents

Acronyms

GDD Gaseous Detector Development

microRWELL micro Resistive Well

triple-GEM triple Gas Electron Multiplier

ASIC Applification-Specific Integrated Circuit

PCB Printed Circuit Board

MPGDs Micro-Pattern Gaseous Detectors

TSV Through Silicon Via

TOT Time over Threshold

TOA Time of Arrival

CERN European Organisation for Nuclear Research

MIP Minimum Ionising Particle

1 Introduction

This project was undertaken as an internship in the Gaseous Detector Development (GDD) group at European Organisation for Nuclear Research (CERN). The group was founded in the 1960s, and in 1968 George Charpak created the multiwire proportional drift chamber[1]. Since then many more gaseous detectors have been built and applied in many different areas in this group. Notable examples include the Gas Electron Multiplier (GEM) and the microRWELL, created in 1997 and 2009 respectively.[2]

Gaseous detectors work by creating primary electron-ion pairs from an incoming photon or minimising ionising particle in the gas, and gathering the electrons by drifting with an electric field. The electrons are also often amplified in areas with very strong electric fields by creating an avalanche effect. Here the electrons gain enough energy to interact with the gas atoms inelastically, and can ionise them to create more electrons. Finally the moving electrons/ions induce a current on the readout electrodes which can be calculated, for example, with the Shockley–Ramo theorem. An in-depth description of how gaseous detectors work can be found in [3].

The report will begin with an overview into the motivations of combining gaseous detectors with a pixelated readout system, as well as the specific aim of this project. Then it will go into the technologies used in the project one-by-one. For each technology, why it was used, the integration process and initial steps relevant to it, as well as some results will be discussed. Finally within each section the conclusions and next steps will be detailed.

2 Motivation

One of the main goals in combining MPGDs with a pixelated readout system is obtaining high spatial resolution tracking with a low material budget. This means that event selection can be gathered based purely on geometry. For example, the event-topology (geometry) event selection can be used in rare event searches such as for recoil dark matter experiments, since gaseous detectors contribute low background and are a light target. There are also applications in x-ray polarimetry, for example as part of the MIXE set-up at the Paul Scherrer Institute (PSI)[4][5]. Combining MPGDs and pixelated readout systems allows for maximum utilisation of the features of both systems. These features are: gaseous detectors have a low-material budget, meaning they are less interactive than other forms of detector. They have easy large area coverage, making them ideal for rare-event searches, they can have high gain, so are sensitive to low energy particles (photons $< 2keV$), and the target density can be adjusted to change the track length of the particle being detected, allowing them more flexibility. Pixelated readout systems have very high spatial and time resolutions, allowing more precise particle tracking in 3 dimensions. They also remove the problem of ghost hits that can occur with strip readout, which is frequently used with gaseous detectors[6].

Being able to use standard Printed Circuit Board (PCB) techniques with this combination would also be beneficial - exploring the possibility of integrating pixelated readout Applification-Specific Integrated Circuit (ASIC)s in gaseous detectors and using standard PCB technologies is a new area that would allow creation of a gas-based amplification stage with a directly embedded readout.

The goal of this project is to take steps towards combining the microRWELL (section 5) with the Timepix4 with TSV (section 3). The reason that these have been chosen will be detailed in each of their technology sections. The steps taken are: analysis, detector characterisation, and simulation.

3 Timepix4

3.1 Timepix4 - The Technology

The ASIC that has been used in the project is the Timepix4[7]. It has many benefits that make it ideal for this project. Firstly, the chip can be bonded to the board through TSV[8], through the back of the chip, meaning that no wire bonds need to be taken care of. This means that a sensor can be embedded directly on-top. TSV as a new technology allows embedding of the microRWELL. This ability to be combined with other sensors (other than silicon) is critical. Additionally, without wire-bonds, the amount of dead

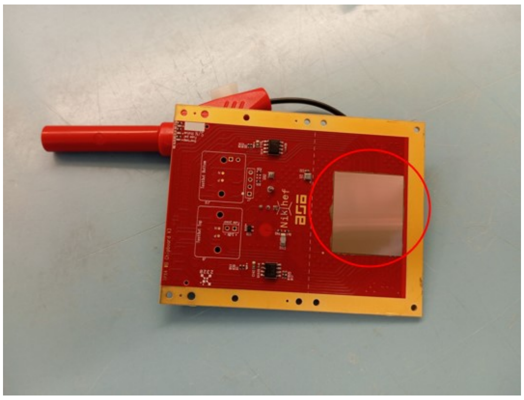

Figure 1: The Timepix4v1 chip with TSV bonded onto the carrier board.

area between chips is reduced, so the chips can form larger arrays with the chips placed directly next to each other. It can be run in both data-driven and frame-based readout modes [9]. It has excellent spacial (55 μm pitch) and time resolution (<200 ps) and rate capability. In data-driven mode, it has a maximum rate of 3.58×10^6 hits /mm^2/s, and in frame-based readout it has a maximum rate of $\sim 5 \times 10^9$ hits /mm^2/s[7]. Finally, the existing family of gaseous detectors with pixelated readouts, for example GEMPix[10] and GridPix[11], already use Timepix.

3.2 Analysis

Reconstruction software for the Timepix4 exists[12], and in this section it was checked to see if this software works for gaseous detector signals with different event signatures between design case and the applications. Thank you to Kevin Heijhoff and Martin van Beuzekom from Nikhef for providing the software.

For one X-ray in silicon sensor you get one pixel hit, and this is ideal for the existing reconstruction software which is based on small numbers of pixels hit. However, in gaseous detectors, the random nature of ionisations and collision leads to spreading out of the initial event, which has to be backtracked through clustering. The purpose of this section was to check how well the existing software (tpx4tools, Nikhef), built for Minimum Ionising Particle (MIP) tracking with silicon sensors in a beam telescope, would perform with the gas detector. At this stage, the Timepix4v1 TSV was not ready for testing, so in order to run the checks, some extended signals (electrons and gammas) were gathered with a ^{90}Sr in a silicon sensor with the Timepix4 without TSV (see figures 2 and 3).

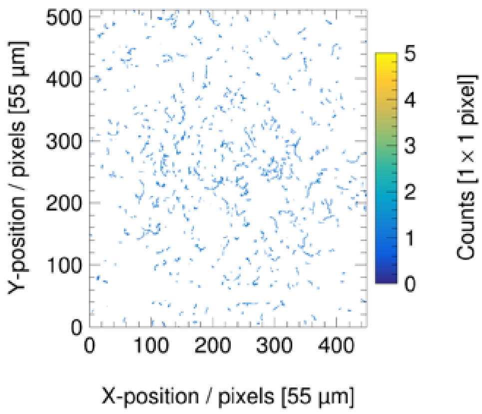

Figure 2: The run that was used in order to emulate gaseous detector signals with the Timepix4 reconstruction software. It was taken using an ^{90}Sr source and a 400 µm silicon sensor with hole collection and 170 V bias voltage, readout out with the Timepix4 (not TSV)

Figure 3: An example electron scattering hit that was used to emulate a gaseous detector signal.

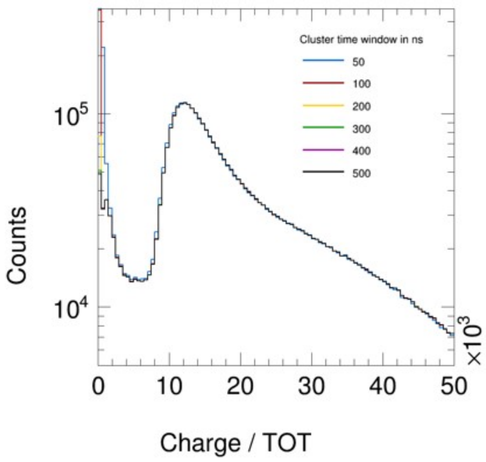

Figure 4: A histogram of charge in units of TOT. This is a spectrum of the ^{90}Sr source that was used to that the image. The spectrum is identical for clustering time windows of 50-500 ns.

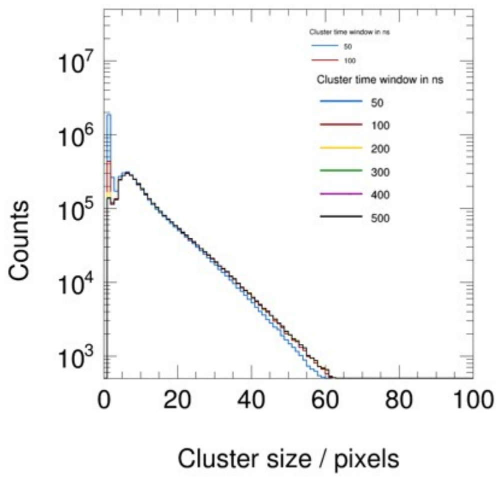

Figure 5: A histogram of cluster size in units of pixels. the cluster size spread is identical for clustering time windows of 50-500 ns.

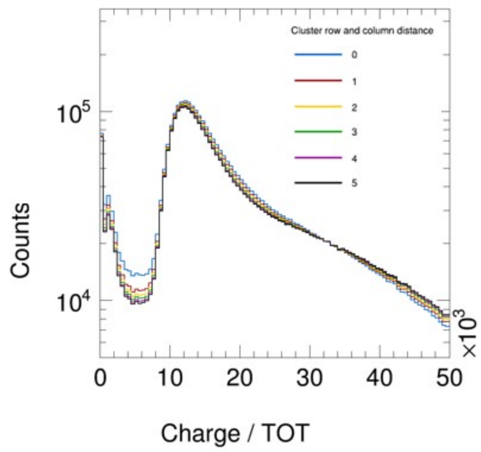

Figure 6: A histogram of charge in units of TOT. This is a spectrum of the ^{90}Sr source that was used to take that the image. The spectrum is identical for clustering pixel sizes of 0-5 pixels.

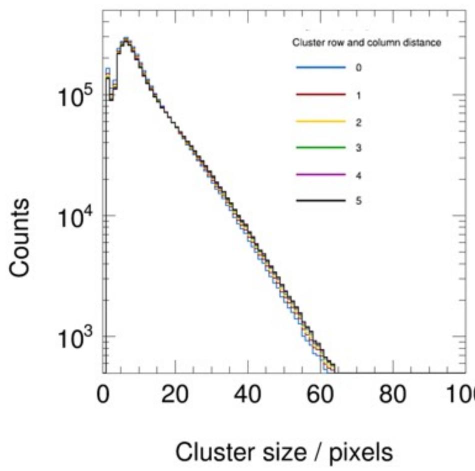

Figure 7: A histogram of cluster size in units of pixels. the cluster size spread is identical for clustering pixel sizes of 0-5 pixels.

From the four graphs in figures 4, 5, 6 and 7, it can be concluded that the current reconstruction software (tpx4tools, Nikhef) is working well within a short time-window (when all the events are counted individually, as can be seen from the individual events in figure 2). The plots in figures 4 and 5 show that clustering time from 50-500 ns has little impact on the clusters that the software reconstructs. This is useful for a gaseous detector because there is inherent spread in arrival time of electrons from the same clustering event due to the random nature of collisions leading to a spread in drift velocity. The plots in figures 6 and 7 show that clustering size in pixels from 0-5 pixels (how many pixels with no hits can be between pixels with positive hits for them to be counted as part of the same cluster) also has minimal impact on clustering ability. This is again useful for a gaseous detector due to the spread in pixel hit locations from a single event.

3.3 Analysis with the Timepix4 - Conclusions and Next Steps

It has been found that the clustering software works also with complex event geometries in silicon detectors and hence should be also suitable for the application with gaseous detectors and their event geometries. However, it still requires verification with the final gaseous detectors results, as found in section 4.2. This may involve re-writing some software in order to get time-stamping and event-clustering working. This will result in being able to obtain the full energy spectra and position reconstruction.

4 Triple-GEM

Before attempting a novel assembly process of embedding the microRWELL on-top of the Timepix4 TSV, the initial step is to check with a more familiar system (the Timepix4 and triple Gas Electron Multiplier (triple-GEM)) that assembly works, and results can be gathered.

4.1 Triple-GEM - The Technology

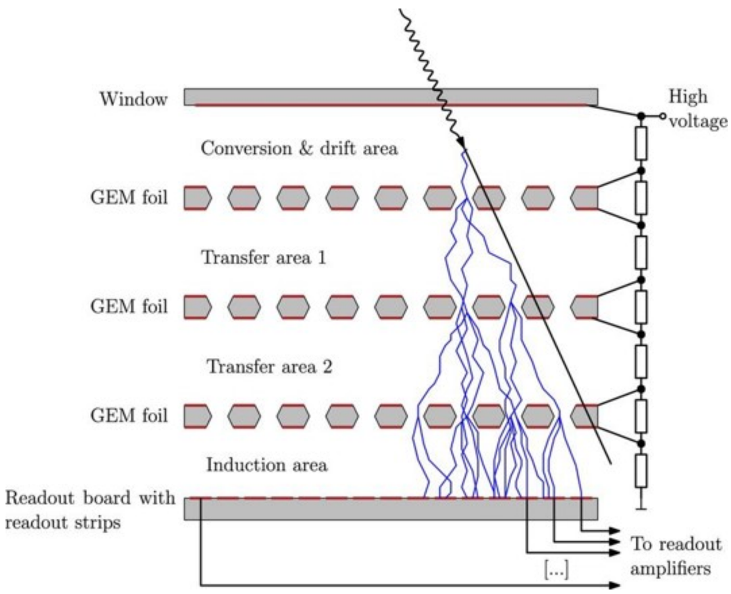

Figure 8: A diagram of the internal structure of the triple-GEM. The three amplification regions in the foils are visible, as well as an example of an incoming photon.[13]

The triple-GEM is three layers of amplification stages (see figure 8) with holes in each layer. Each layer (a GEM) has a voltage applied across it between copper electrodes, with a kapton layer in-between. Triple-GEMs can achieve higher gain than GEMs due to the multiple amplification regions in the holes, which is why the triple-GEM has been used instead of a single layer GEM in this project. Additionally, the triple-GEM has been used in combination with previous versions of the Timepix already[10].

4.2 Detector Characterisation and Assembly

As a first stage, a gain curve was measured with a single channel anode, as shown in figure 9, to then apply this knowledge in the tests when the Timepix4 is attached to understand what gains can be achieved without discharges that could damage the Timepix4. When the triple-GEM was combined with the Timepix4v1 TSV, the detector was operated at a divider voltage (see Appendix 8.2 for a divider scheme) of 3900 V, at a gain of 2500.

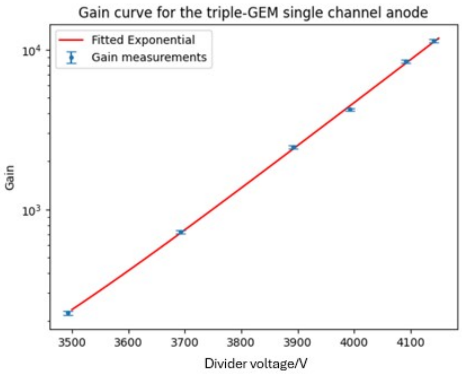

Figure 9: A gain curve taken from a divider voltage of 3500 V to 4100 V, covering a gain of 1000-10000. This was taken with the triple-GEM on-top of a single-channel anode.

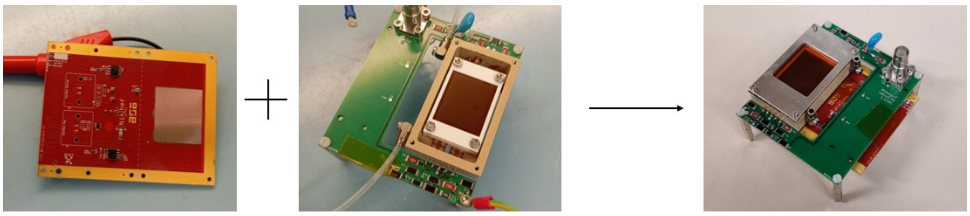

Figure 10: Images of the assembly of the triple-GEM on-top of the Timepix4 readout system. Timepix4v1 on the left, triple-GEM on the right, with the assembled detector as the result.

Then the triple-GEM and Timepix4v1 (TSV) were assembled, as can be seen in figure 10. This allowed testing of the readout of the Timepix4 with a gaseous detector for which pixelated readout has previously been successful, for example the GEMPix[10], and for which simulations exist.
The results of assembly and then a 5 second run taken with ^{90}Sr source is shown in figure 11. The X-ray image taken over 25 minutes with a pen is shown in figure 12. The outline of the pen in the longer run can clearly be seen, as well as individual events in the shorter one. The assembly process has worked, with clear long images and individual events visible in each image respectively. The image-taking process can now be refined by using fast readout links to avoid bandwidth congestion and removing any noise in post-processing. The initial results (pre-equalisation checks) can be found in the appendix, section 8.1, as demonstration of the steps taken to get to these images.

4.3 Detector assembly and characterisation with the triple-GEM and Timepix4 - Conclusions and Next Steps

Images have been successfully taken with this combination of technologies. There are some vertical lines in the bottom right-hand quadrant of figure 12, but with a faster readout system, and therefore more bandwidth available, this will likely disappear. In the results taken so far, the data was read-out using the slow links on the Timepix4v1 TSV. These run at 40 Mb per second. This limits the rate capabilities of this system, and so the next step for this section is to get the fast links running with the Timepix4v1 TSV using the Nikhef software, which will likely remove the vertical lines.

5 microRWELL

5.1 microRWELL - The Technology

The microRWELL is made from a copper electrode on the top, kapton wells, and then a resistive layer underneath (see figure 13). It has the ability to be placed directly on top of a chip, which is important

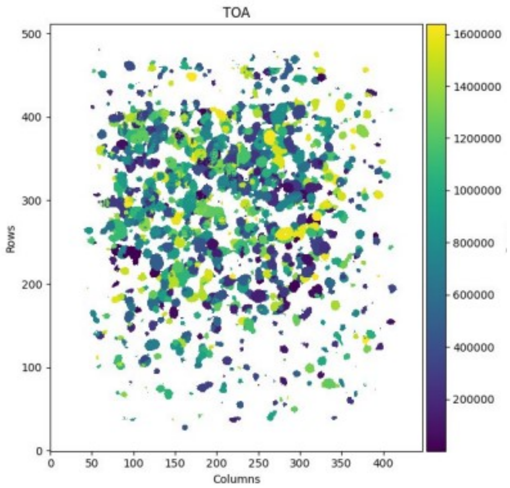

Figure 11: A TOA image taken in a 5 second run with the Timepix4v1 TSV underneath the triple-GEM, with ^{90}Sr source. The individual hits are clear in the TOA plot. The colourmap is TOA in arbitrary units.

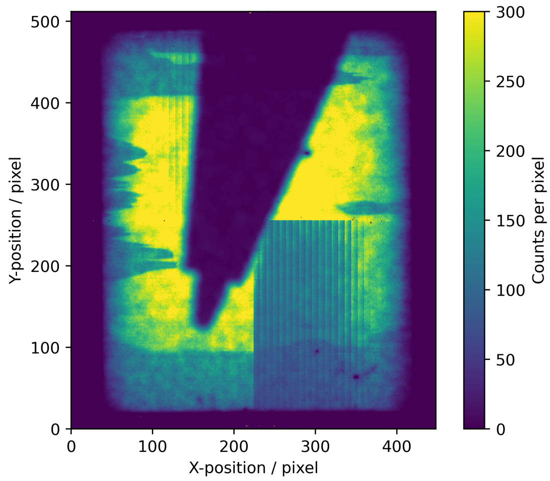

Figure 12: A hitmap image taken in a 25 minute run with the Timepix4v1 TSV underneath the triple-GEM, with ^{55}Fe source above a pen. Without flat field correction.

when embedding it. It is the microRWELL that is wanted to combine with the Timepix4 as an end-result for a few reasons. The first reason is that it has a lower material budget than the triple-GEM because it has only one amplification stage, and no transfer or induction regions. One of the main goals of this project is to create a high resolution detector with a low material budget, so the microRWELL is ideal for this. Also, it is easy to produce using standard PCB techniques. In addition, it protects the Timepix4 from discharge because of the presence of the resistive layer which quenches the discharges and insulating kapton, which prevents any charge flowing to the chip. This means that the detector can be operated at high gains, without damaging the chip.

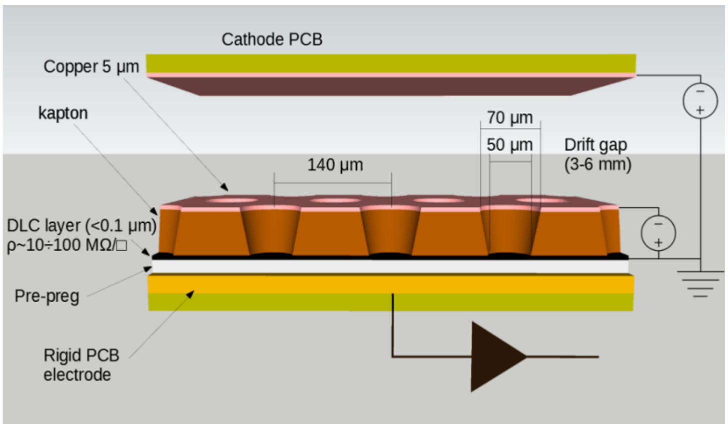

Figure 13: A diagram of the internal structure of the microRWELL, not to scale.[14] There is a copper electrode, kapton wells where the amplification occurs, a resistive layer, and then the readout electrode underneath.

5.2 Simulation

In order to progress towards the goal of embedding the microRWELL on-top of the Timepix4, simulation was performed in order to track the signal coupling from the microRWELL to the readout pads. This provides an expectation of the functionality and expectations for the results post-assembly.

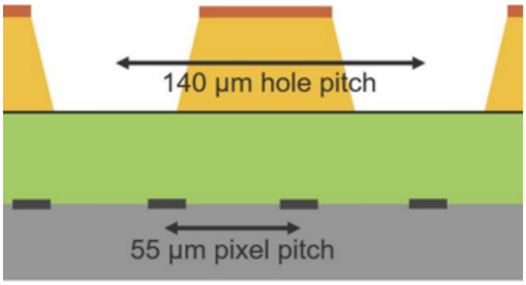

Figure 14: The geometry of the microRWELL to scale, in order to show the difference between the hole pitch and size, and the readout pad pitch and size.

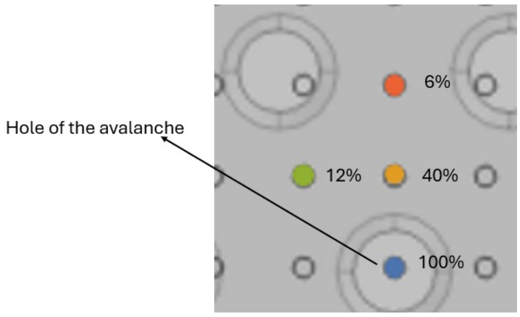

Figure 15: A diagram of the simulation - an electron is put through the avalanche hole and the charge is read-out in 4 pads. One pad directly underneath, and then 3 pads in ascending distance. (blue 1 - yellow 2 - green 3 - red 4). The percentages are the maximum charge read out as a percentage of the blue central pad.

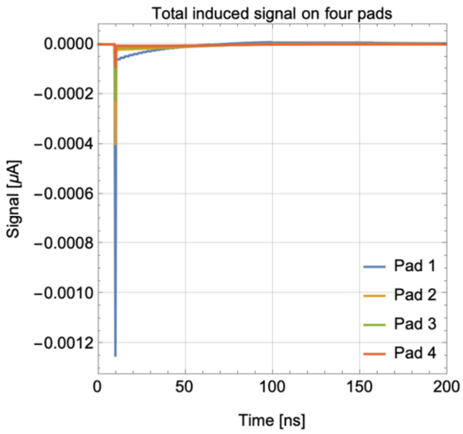

Figure 16: The results of the simulation - total induced signal on four pads.

As can be seen in figure 14, the pitch and size of the kapton holes in the microRWELL is different to the aluminium readout pads. The simulations allow understanding and estimation of the signal coupling between the different geometries of the readout pads and amplification holes.

In the simulations the case of one electron entering one hole and being amplified has been covered, and from this the 4 nearby readout pads were looked at to see the signal readout on each (see figure 15). Figure 16 shows the total induced signal on four pads. As expected, the largest maximum signal is induced on the blue pad 1 right below the hole, with yellow pad 2 being the second largest signal, green pad 3 the next, and red pad 4 the smallest signal since it is furthest away. The yellow pad 2 receives 40% of the maximum charge readout from the blue pad 1, green pad 3 15.2%, and red pad 4 6%. This means that charge information could be lost based on the hole-readout-pad geometry, however not conclusively at this stage. And even if charge information is lost, iit will likely not impact the function of the detector.

5.3 Simulation with the microRWELL - Conclusions and Next Steps

The simulations have confirmed that it is worth proceeding with the assembly process, although more simulations will likely be done to better understand the signal coupling quantitatively. So the next step for the assembly is as follows: place the microRWELL ontop of the Timepix4 TSV. By placing the microRWELL on-top of the Timepix4v1 TSV, the electric fields between the resistive layer and the anode will keep it in place with minimal gapping. This will allow tests of signal coupling and detector characteristics before full embedding occurs.

6 Summary and Conclusion

The goal of this project was to take steps towards taking the first images with the Timepix4 TSV and a gaseous detector. This project was successful in this goal. The Timepix4 section (3) showed that the existing reconstruction software for the Timepix4 that was built for MIP tracking with silicon sensors works for extended electron and gamma signals in a silicon sensor, and thus will work for gaseous detector signals. This is also useful for various detector-based groups being able to collaborate and accelerate developments in the future. The simulation with the microRWELL and readout pads shows that despite a possible signal loss because of the induction process, there is still enough charge information to have a fully functioning detector. And finally, the very first images in the world were taken with the Timepix4 TSV. This is all very encouraging for using and developing this technology in the future.

The three stages - analysis, detector characterisation and assembly, and simulation - all lead to the same conclusion: the integration process aiming to embed the microRWELL with the Timepix4v1 with TSV can, and should, continue.

7 Acknowledgements

Thank you to my supervisors Lucian Scharenberg and Florian Brunbauer for all their help over the past 8 weeks. And an extended thank you to all the other members of the GDD group for being so friendly and helpful. Thank you to Jerome Alozy for his help in obtaining the Timpepix4v1 TSV, as well as Mateus Vicente for bonding the TSV chips on the carrier boards. Thank you to Xavi Llopart for his help in connecting and communicating with the Timepix4 chip. Thank you to Pierre Carbonez and Tristan Genetay for their help in getting the results from the detector. And thank you to Djunes Janssens for his help with the simulation studies.

References

[1] Charpak, G., & Sauli, F. (1979). Multiwire proportional chambers and drift chambers. Nuclear Instruments and Methods, 162(1–3), 405–428. https://doi.org/10.1016/0029-554x(79)90726-2

[2] GDD. https://gdd.web.cern.ch/

[3] Sauli, F. (2014). Gaseous radiation detectors: Fundamentals and Applications. Cambridge University Press.

[4] Prokscha, T. (2022, March 15). MUOn Induced X-ray Emission (MIXE) Project. PSI. https://www.psi.ch/en/smus/muon-induced-x-ray-emission-mixe-project

[5] Žemlička, J., Jakůbek, J., Kroupa, M., & Tichý, V. (2009). Energy- and position-sensitive pixel detector Timepix for X-ray fluorescence imaging. Nuclear Instruments and Methods in Physics Research Section a Accelerators Spectrometers Detectors and Associated Equipment, 607(1), 202–204. https://doi.org/10.1016/j.nima.2009.03.140

[6] Gnanvo, K., Lee, S. J., Mehl, B., De Oliveira, R., & Weisenberger, A. (2024). Performance of a triple-GEM detector with capacitive-sharing 3-coordinate (X–Y–U)-strip anode readout. Nuclear Instruments and Methods in Physics Research Section a Accelerators Spectrometers Detectors and Associated Equipment, 1066, 169654. https://doi.org/10.1016/j.nima.2024.169654

[7] Llopart, X., Alozy, J., Ballabriga, R., Campbell, M., Casanova, R., Gromov, V., Heijne, E., Poikela, T., Santin, E., Sriskaran, V., Tlustos, L., & Vitkovskiy, A. (2022). Timepix4, a large area pixel detector readout chip which can be tiled on 4 sides providing sub-200 ps timestamp binning. Journal of Instrumentation, 17(01), C01044. https://doi.org/10.1088/1748-0221/17/01/c01044

[8] What are Through-Silicon vias? (n.d.). https://resources.system-analysis.cadence.com/blog/what-are-through-silicon-vias

[9] Qd-Admin. (2024, May 24). Frame-based and event-based detection explained. Quantum Detectors. https://quantumdetectors.com/frame-based-and-event-based-detection-explained/

[10] GEMPIX — Knowledge Transfer. (n.d.). https://knowledgetransfer.web.cern.ch/technologies/gempix

[11] Van Der Graaf, H. (2007). GridPix: An integrated readout system for gaseous detectors with a pixel chip as anode. Nuclear Instruments and Methods in Physics Research Section a Accelerators Spectrometers Detectors and Associated Equipment, 580(2), 1023–1026. https://doi.org/10.1016/j.nima.2007.06.096

[12] https://gitlab.cern.ch/TimepixTelescope/tpx4tools

[13] Zabołotny, W.M., Kasprowicz, G., Poźniak, K. et al. FPGA and Embedded Systems Based Fast Data Acquisition and Processing for GEM Detectors. J Fusion Energ 38, 480–489 (2019). https://doi.org/10.1007/s10894-018-0181-2

[14] Farinelli, R., Amoroso, A., Balossino, I., Bencivenni, G., Bertani, M., Cafaro, V., Cibinetto, G., De Lucia, E., Dominici, D., Evangelisti, F., Felici, G., Gatta, M., Garzia, I., Giacomelli, P., Giovannetti, M., Gramigna, S., Lavezzi, L., Melchiorri, M., Mezzadri, G., . . . Sosio, S. (2023). The μ-RWELL technology for the preshower and muon detectors of the IDEA detector. Nuclear Instruments and Methods in Physics Research Section a Accelerators Spectrometers Detectors and Associated Equipment, 1048, 167993. https://doi.org/10.1016/j.nima.2022.167993

8 Appendix

8.1 Initial images taken with the triple-GEM and Timepix4v1 TSV

The very first images taken with the Timepix4v1 TSV and the triple-GEM mounted on top were very noisy. In figure 17, the background image can be seen, and this shows clear vertical lines that have no set-up-based explanation for existing, so were concluded to be due to noise. The noise in the initial images in the chip (figures 17 and 18) was found to be coming from the equalisation procedure used. The equalisation was initially being done in event-based (data-driven) mode, which lead to congestion of the bandwidth in slow link mode due to noisy pixels around the periphery in the Timepix4v1.

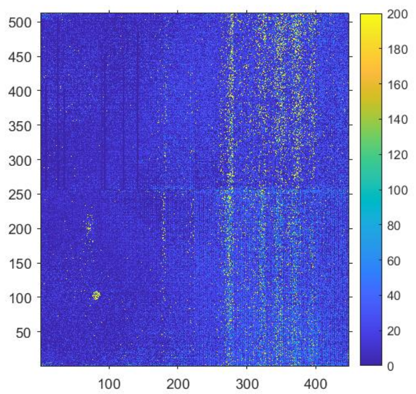

Figure 17: An image taken over 60 seconds with no source present. Taken with triple-GEM placed on top of Timepix4 with TSV.

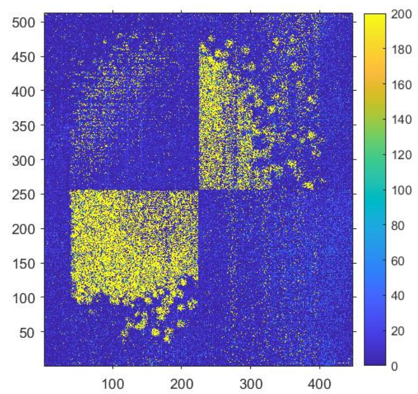

Figure 18: An image taken over 60 seconds with ^{55}Fe 15kHz source present. Taken with triple-GEM placed on top of Timepix4 with TSV, and then the background in figure 17 subtracted in post-processing.

The pixels are read-out in 2 strips (split horizontally), the bottom is read out from the left, and the top is read out from the right, which can be seen in the quadrant-pattern and can explain why the circular result that was expected did not appear. From these results, the equalisation procedure was changed to frame-based mode, and this resulted in the successful images shown in figures 11 and 12.

The circular clusters in figure 18 are also a surprising feature, since the source is at a rate of 15kHz, and over a 60 second run, no individual hits should be visible. This problem was also solved when the equalisation was changed to a frame-based scheme.

8.2 Divider scheme

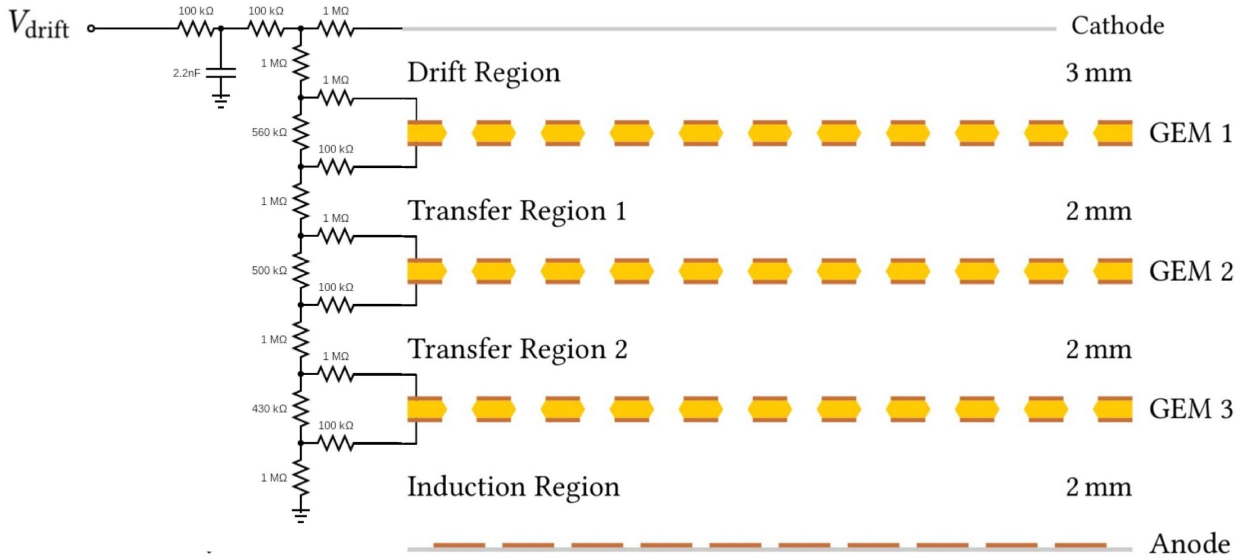

Figure 19: A diagram of the divider scheme of the triple-GEM.